Recruitment of TLR adapter TRIF to TLR4 signaling complex is mediated by the second helical region of TRIF TIR domain

Wenji Piao[a], Lisa W. Ru[a], Kurt H. Piepenbrink[b], Eric J. Sundberg[b,c,d], Stefanie N. Vogel[a], and Vladimir Y. Toshchakov[a,1]

Departments of [a]Microbiology and Immunology, [c]Medicine, and [d]Microbiology and Immunology, and [b]Institute of Human Virology, University of Maryland School of Medicine, Baltimore, MD 21201

Edited by Shizuo Akira, Osaka University, Osaka, Japan, and approved October 11, 2013 (received for review July 17, 2013)

Toll/IL-1R resistance (TIR) domain–containing adapter-inducing IFN-β (TRIF) is a Toll-like receptor (TLR) adapter that mediates MyD88-independent induction of type I interferons through activation of IFN regulatory factor 3 and NFκB. We have examined peptides derived from the TRIF TIR domain for ability to inhibit TLR4. In addition to a previously identified BB loop peptide (TF4), a peptide derived from putative helix B of TRIF TIR (TF5) strongly inhibits LPS-induced cytokine and MAPK activation in wild-type cells. TF5 failed to inhibit LPS-induced cytokine and kinase activation in TRIF-deficient immortalized bone-marrow–derived macrophage, but was fully inhibitory in MyD88 knockout cells. TF5 does not block macrophage activation induced by TLR2, TLR3, TLR9, or retinoic acid-inducible gene 1/melanoma differentiation-associated protein 5 agonists. Immunoprecipitation assays demonstrated that TF4 binds to TLR4 but not TRIF-related adaptor molecule (TRAM), whereas TF5 binds to TRAM strongly and TLR4 to a lesser extent. Although TF5 prevented coimmunoprecipitation of TRIF with both TRAM and TLR4, site-directed mutagenesis of the TRIF B helix residues affected TRIF–TRAM coimmunoprecipitation selectively, as these mutations did not block TRIF–TLR4 association. These results suggest that the folded TRIF TIR domain associates with TRAM through the TRIF B helix region, but uses a different region for TRIF–TLR4 association. The B helix peptide TF5, however, can associate with either TRAM or TLR4. In a mouse model of TLR4-driven inflammation, TF5 decreased plasma cytokine levels and protected mice from a lethal LPS challenge. Our data identify TRIF sites that are important for interaction with TLR4 and TRAM, and demonstrate that TF5 is a potent TLR4 inhibitor with significant potential as a candidate therapeutic for human sepsis.

signaling complex assembly | TLR4 targeting | TIR domain recognition site | decoy peptides

Toll-like receptors (TLRs) initiate innate immune responses by recognizing specific pathogen-associated molecules; for example, TLR4 recognizes lipopolysaccharides (LPSs) of Gram-negative bacteria (1, 2). Ligand recognition induces dimerization of cytoplasmic Toll/IL-1R resistance (TIR) domains of two receptor molecules and causes recruitment of intracellular TIR domain-containing adapters. Four adapter proteins participate in TLR4 signaling: myeloid differentiation factor 88 (MyD88) (3), TIR domain-containing adapter protein, also known as MyD88-adapter-like (TIRAP–Mal) (4, 5), TIR domain–containing adapter-inducing IFN-β, also known as TLR adaptor molecule 1 (TRIF–TICAM-1) (6, 7), and TRIF-related adaptor molecule also known as TLR adaptor molecule 2 (TRAM–TICAM-2) (8, 9). TIRAP–Mal is important for MyD88 recruitment to the signaling complex located at the plasma membrane to initiate early NF-κB and mitogen-activated protein kinase (MAPK) activation and induce "MyD88-dependent" proinflammatory cytokines, such as TNF-α and IL-1β (4, 5, 10). TRAM is important for TRIF recruitment to the endosomally located TLR4 signaling complexes to activate IFN regulatory factor 3 (IRF3) and induce IRF3-dependent cytokines, such as IFN-β and RANTES (regulated upon activation normal T-cell expressed and secreted) (8, 9, 11).

A typical TIR domain consists of the central five stranded parallel β sheets (the strands are designated as βA–βE) surrounded by 5 α-helices (i.e., αA–αE) (12, 13). The TIRAP–Mal TIR domain has an atypical fold compared with other resolved mammalian TIR structures in that the position of its β-strand B is shifted by 12–18 amino acids toward the C terminus, so that TIRAP TIR does not have a helix B but has an unusually long AB loop (14, 15). Structures of the TIR domains of TLR4, TRIF, and TRAM have not been yet resolved. The TIR domain is a key structural feature present in all TLRs and TLR adapter proteins. TIR domains mediate transient homotypic or heterotypic protein interactions required for agonist-driven assembly of TLR signaling complexes (13, 16, 17). Multiple interactions of TIR domains of TLRs and TLR adapters are required to mediate adapter recruitment and stabilize initial complex (18–20). It has been proposed that TLR4 activation leads to formation of several compositionally distinct complexes. Kagan et al. proposed that TLR4 engages TIRAP–MyD88 and TRAM–TRIF sequentially at distinct cellular locations (11), thus implying that the two sets of adapters may compete for the same binding site at the TLR4 homodimer. However, it remains unclear how exactly the four adapters interact with each other and TLR4 to orchestrate TLR4 signaling.

The presumed mechanism of signaling inhibition by a decoy peptide is that the peptide competes with its prototype protein for the prototype's docking site and thereby prevents a protein–protein interaction required for signaling (19). In this study, we have examined cell-permeable decoy peptides derived from the TIR domain of TRIF. Two peptides, TF4 and TF5, from the

Significance

This study sheds light on the mechanisms of Toll-like receptor 4 (TLR4) signaling complex assembly. Particularly, the interaction site that mediates Toll/IL-1R resistance (TIR) domain–containing adapter-inducing IFN-β (TRIF) recruitment to the TLR4 signaling complex is identified within the second helical region of the TRIF TIR domain. This finding is significant because "a mimic" of this site potently inhibits TLR4 signaling in cells by a competitive mechanism and decreases LPS-induced mortality in mice by more than 80%.

Author contributions: V.Y.T. conceived the idea and designed the set of peptides; W.P., S.N.V., and V.Y.T. designed research; W.P., L.W.R., and K.H.P. performed research; S.N.V. contributed new reagents/analytic tools; K.H.P. and E.J.S. obtained and analyzed data on peptide structure; and W.P., S.N.V., and V.Y.T. wrote the paper.

Conflict of interest statement: V.Y.T. has a patent pending for targeting TLR4 signaling by TRIF peptides.

This article is a PNAS Direct Submission.

[1]To whom correspondence should be addressed. E-mail: vtoshchakov@som.umaryland.edu.

This article contains supporting information online at www.pnas.org/lookup/suppl/doi:10.1073/pnas.1313575110/-/DCSupplemental.

second loop (BB loop) and the second helical region (helix B) of the TRIF TIR, respectively, potently inhibited LPS-induced activation of MAPKs and induction of MyD88-dependent and TRIF-dependent cytokines in wild-type macrophages. TF5 did not inhibit TLR4 signaling in TRIF$^{-/-}$ immortalized bone-marrow–derived macrophages (iBMDMs) but did exhibit full activity in the MyD88$^{-/-}$ cells. TF5 inhibits TLR4-driven macrophage signaling at a lower dose in vitro compared with TF4 and binds to both TRAM and TLR4, whereas TF4 targets TLR4 but not the TRAM TIR. In a mouse model of TLR4-driven inflammation, TF5 potently decreased the systemic cytokine levels induced in mice by a sublethal LPS dose, and dramatically improved survival of mice challenged with a lethal LPS dose.

Results

Peptides Derived from the BB Loop (TF4) and B Helix (TF5) of TRIF TIR Inhibit TLR4-Mediated Macrophage Activation. The TRIF-derived peptide library was designed similarly to the TLR4, TIRAP, and TRAM libraries as reported previously (20–22). Sequences of TRIF peptides are provided in Table S1. Each peptide was synthesized contiguously with the cell-permeating sequence of *Antennapedia* homeodomain (RQIKIWFQNRRMKWKK) (Antp) (23) located at the N terminus. Peptide effects on LPS-induced cytokine mRNA expression were first measured. Murine peritoneal macrophages were pretreated with peptides at 5 or 20 μM for 30 min and then stimulated with LPS (100 ng/mL) for 1 or 5 h. TF5, a decoy peptide derived from the B helix of TRIF TIR, was most inhibitory among TRIF peptides; it potently inhibited the LPS-induced mRNA expression of MyD88-dependent (e.g., TNF-α and IL-1β) as well as "TRIF-dependent" (e.g., IFN-β and RANTES) cytokines, even at the lower dose of 5 μM (Fig. 1*A*). Another inhibitory peptide, TF4, was derived from the BB loop of TRIF TIR. This peptide was identified as moderately inhibitory in our earlier study that compared peptides derived from BB loops of four TLR adapters (24). TF4 was effective only at the higher dose of 20 μM (Fig. 1 *A*–*C*). IL-6 is induced later than the other cytokines studied; therefore, IL-6 expression was measured 5 h poststimulation. IL-6 mRNA expression was suppressed markedly by TF5 at 5 μM and TF4 at 20 μM (Fig. 1*A*). We next examined the effect of these TF4 and TF5 inhibitory peptides on TLR4-mediated cytokine secretion. Macrophage supernatants were collected 24 h after LPS stimulation, and cytokine protein levels (e.g., TNF-α, IL-6, IFN-β, RANTES) were measured by ELISA. IL-1β was measured in cell lysates. Consistent with the effect of peptides on cytokine gene expression, TF5 exerted a stronger inhibitory effect on production of all five cytokines examined, whereas TF4 inhibited less efficiently (Fig. 1*B*).

The effects of TRIF peptides on MAPK activation (p38, ERK, and JNK) were also examined. Murine macrophages were pretreated with peptides for 30 min, stimulated with LPS, and lysed 30 min poststimulation. Consistent with peptide effects on cytokine mRNA expression, both TF5 and TF4 blocked the activation of all three MAPKs at 20 μM (Fig. 1*C*). Inhibitory TRIF peptides did not affect cell viability in the MTT (3-(4,5-Dimethylthiazol-2-yl)-2,5-diphenyltetrazolium bromide) viability assay that involved a 2 h incubation and concurrent stimulation of cells with LPS (Fig. S1*A*), indicating that the inhibition was not due to cellular toxicity. The peptides were also tested for their possible agonist activity. Except for TF11, the peptides did not activate p38 MAPK (Fig. S1*B*). LPS induces STAT1-Y701 phosphorylation through autocrine activation of type I IFN receptor by IFN-β (25). Fig. 1*D* demonstrates that TF5 efficiently blocks IFN-β response and abolishes STAT1-Y701 phosphorylation.

Structural Analysis of TF4 and TF5 Peptides. We used circular dichroism (CD) spectroscopy to analyze solution structures of inhibitory TRIF peptides. Because peptides contain a common *Antennapedia* homeodomain internalization sequence, Antp, TF4, and TF5 spectra were referenced against that of Antp to enable deduction of structures of TRIF-specific parts of these peptides. The spectra of TF4, TF5, Antp, and the Antp-referenced spectra of TF4 and TF5 are shown in Fig. S2. Antp peptide is known to be disordered in aqueous solutions and adopt an α-helical structure in less polar environments or upon binding to lipid membranes (26–28). According to our data analyzed by K2d algorithm (29), Antp is 7% α helical, 51% β strand, and 42% coil. This structure is consistent with findings of Czajlik et al. and Chrisiaens et al., who found that Antp in aqueous solution is 11% and 10% α helical, respectively (27, 28). Analysis of the Antp-referenced TF4 spectrum suggested that the decoy part of TF4 is predominantly a coil, as the peptide is 2% α helical, 17% β strand, and 81% coil. Similar analysis suggested that the decoy part of TF5 is 27% α helical, 32% β strand, and 41% coil. Thus, TF5 appears to be more helical in solution than TF4, yet the coiled conformation predominates in the solution structure of both peptides. Similar results were obtained using the Self-Consistent Method algorithm (SELCON3) (30). These findings agree with the notion that peptides derived from a natural protein tend to prefer the conformation they assume in the context of the folded protein

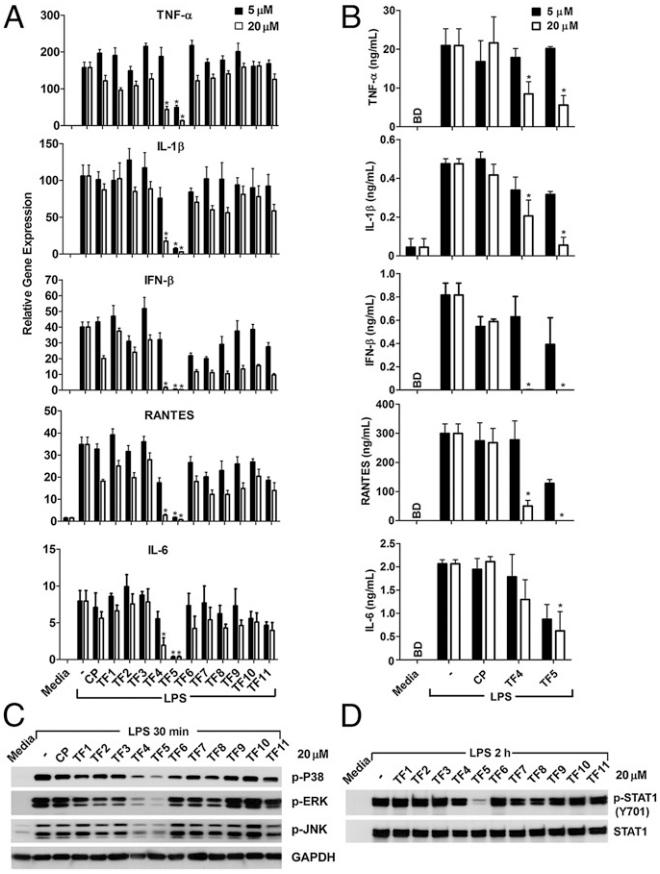

Fig. 1. Peptides derived from the BB loop (TF4) and B helix (TF5) of TRIF TIR inhibit TLR4-mediated macrophage activation. (*A* and *B*) Mouse peritoneal macrophages were incubated with 5 (black bars) or 20 (open bars) μM of indicated peptides for 30 min before LPS stimulation (100 ng/mL). (*A*) Cytokine mRNA expression was measured by real-time PCR 1 h (TNF-α, IL-1β, IFN-β, and RANTES) or 5 h (IL-6) after LPS stimulation and was normalized to the expression of the *Hprt* housekeeping gene. (*B*) Supernatants were collected 24 h after LPS stimulation and analyzed for TNF-α, IL-6, IFN-β, and RANTES by ELISA. IL-1β was measured in cell lysates. Means ± SEM of three independent experiments are shown in *A* and *B*. *$P < 0.01$. (*C* and *D*) Cell lysates were analyzed for activated forms of MAPKs or STAT1 30 min or 2 h after LPS stimulation, respectively. *C* and *D* represent one of three separate experiments. BD, below detection limit; CP, control peptide.

because packing in natural proteins is, in general, energy-optimized; yet peptides also demonstrate a higher degree of structural heterogeneity due to higher mobility of their termini (31).

Specificity of TLR4 Inhibition by TRIF Peptides. The specificity of TLR4 inhibition by TRIF peptides was studied next. TF3 was used as a noninhibitory control peptide in these experiments. TF4 inhibited IFN-β mRNA transcription in mouse macrophages stimulated with poly (I:C) (50 μg/mL) for 5 h (Fig. S3*A*). However, the inhibition of IFN-β mRNA was relatively weak and did not prevent the TLR3-induced phosphorylation of STAT1-Y701 (Fig. S3*C*). In sharp contrast with the potent inhibition of TLR4-mediated macrophage activation, neither TF4 nor TF5 affected induction of TNF-α and IL-1β mRNA, or MAPK phosphorylation induced by TLR2 agonists P3C or P2C (Fig. S3 *B* and *D*). Neither TLR9– nor retinoic acid-inducible gene 1- (RIG-I)–like receptor-mediated IFN-β activation induced by oligonucleotide (ODN) 1668 and poly (I:C) LyoVec, respectively, was affected by TF4 or TF5 (Fig. S3 *A* and *C*).

Peptide Derived from the Conserved Segment of TF5 Efficiently Inhibits TLR4 in Mouse and Human Cells. The putative B helix of the TRIF TIR domain is conserved in mice and humans. Nine consecutive N-terminal amino acids of the region represented by TF5 are identical in both species. Thus, we next compared the inhibitory efficiency of original TF5 (CLQDAIDHSGFT) with that of the conserved part of TF5, CLQDAIDHS (TF5-ΔC), and the homologous sequence derived from the human TRIF, CLQDAIDHSAFI (hTF5). All three peptides potently inhibited LPS-induced cytokine and MAPKs activation in primary mouse macrophages (Fig. 2 *A* and *B*) and differentiated THP-1 cells (Fig. 2 *D* and *E*), thereby suggesting that nine N-terminal amino acids are responsible for TLR4 inhibition by TF5.

Inhibition of TLR4 by TF5 Is TRIF-Dependent. Next, we studied how TRIF peptides, which are inhibitory in wild-type cells, affect TLR4 signaling in TRIF- and MyD88-deficient cells. TF5 and TF5-ΔC inhibited activation of TLR4 in wild-type iBMDMs as potently as in wild-type peritoneal macrophages (Figs. 1 *A* and *C* and 2 *F* and *H*). In remarkable contrast with this observation, TF5 and TF5-ΔC neither prevented activation of TNF-α and IL1-β in TRIF-deficient iBMDM (Fig. 2*F*) nor inhibited MAPK or IkB kinase (IKK)-α/β phosphorylation (Fig. 2*H*). Interestingly, TF5 retained full inhibitory activity in MyD88-deficient peritoneal macrophages (Fig. 2 *G* and *I*). These data strongly suggest that TF5 targets a protein of the TRIF-dependent pathway, with TRAM being the most likely target candidate.

TF4, a weaker inhibitor of TLR4 in wild-type macrophages, did not inhibit TNF-α and IL-1β in iBMDMs (Fig. 2*F*), perhaps due to differences in cell background. Therefore, it is hard to tell whether inhibition of these genes by TF4 is TRIF pathway–dependent; yet it should be noted that IFN-β and RANTES are more weakly inhibited by TF4 in MyD88-deficient macrophages compared with wild-type cells (Fig. 2*G*). Absence of IFN-β mRNA induction in TRIF-deficient cells (Fig. 2*F*) and weak induction of IL-1β mRNA in MyD88-deficient cells (Fig. 2*G*) are shown to confirm cell phenotypes.

TF5 Binds Both TRAM and TLR4 and Blocks Both TRIF–TRAM and TRIF–TLR4 Coimmunoprecipitation, Whereas TF4 Binds TLR4 Selectively and Blocks Only TRIF–TLR4 Association. To understand the specificity of TLR4 targeting by TF4 and TF5, we conducted dot blot peptide binding assays. Lysates of HEK293T cells expressing Flag-tagged TLR4 or TRAM were incubated with 20 μM of TF4 or TF5 for 1 h and then immunoprecipitated with anti-Flag antibody. The precipitates were analyzed by dot blotting for TF4 and TF5 using an antibody to the translocating segment of *Antennapedia*, present on both peptides. Peptide 4BB was used as a positive binding control for TLR4, as we previously demonstrated strong

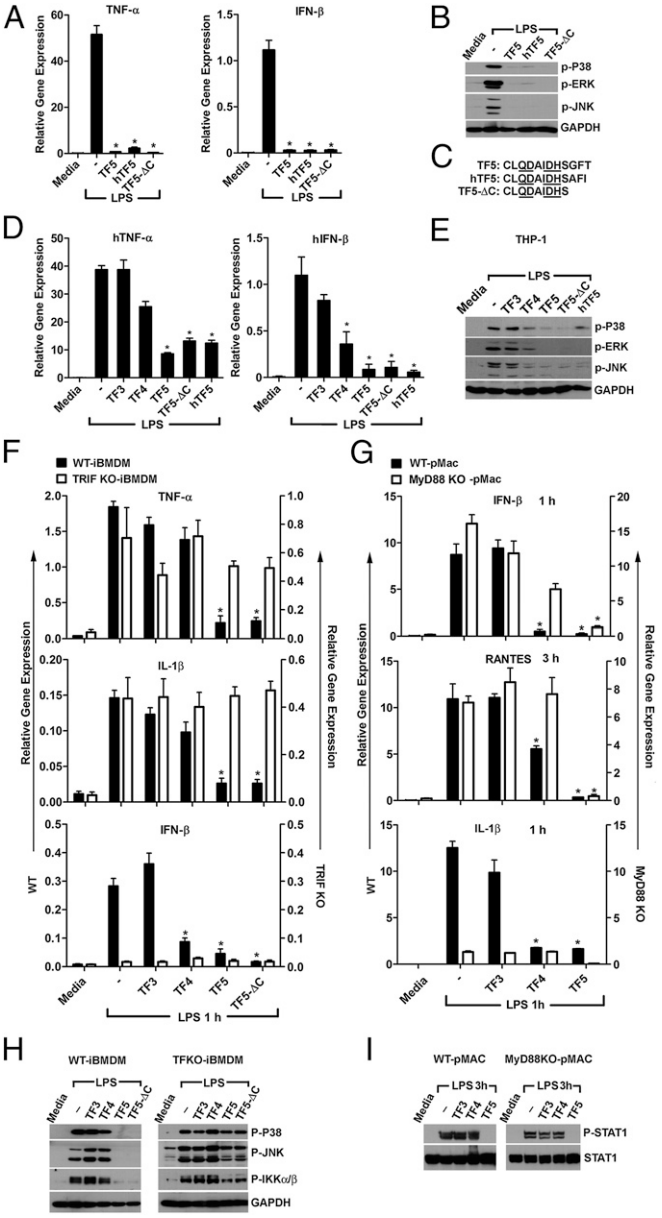

Fig. 2. Conserved segment of TF5 inhibits TLR4 in mouse and human cells. TLR4 inhibition by TF5 is TRIF-dependent. Experimental details are as in Fig. 1. We preincubated 2×10^6 mouse wild-type (*A* and *B*) or MyD88-deficient (*G* and *I*) peritoneal macrophages or differentiated THP-1 cells (*D* and *E*) or wild-type or TRIF-deficient iBMDMs (*F* and *H*) with 20 μM of indicated peptides for 30 min and stimulated them with LPS (100 ng/mL). (*A*, *D*, and *F*) LPS-induced TNF-α, IL-1β, and IFN-β mRNA were measured 1 h after LPS challenge. RANTES mRNA (*G*) and phospho–STAT-1 (*I*) was measured 3 h post-stimulation. Means ± SEM of three independent experiments are shown. $^*P < 0.01$. (*B*, *E*, and *H*) MAPKs and IKK activation was measured 30 min after LPS stimulation. Western blots shown represent three separate experiments. The sequences of human and murine TF5 and TF5-ΔC are presented in *C*.

binding for this peptide–protein pair by FRET (20). Data suggest that TF5 binds to TLR4 and TRAM, whereas TF4 binds only to TLR4 and not TRAM. Binding of TF4 to TLR4 was consistently stronger than TF5 but weaker than 4BB (Fig. 3*A*). The noninhibitory peptide TF3 did not bind TLR4 or TRAM (Fig. 3 *A* and *B*). Thus, this analysis suggests that TLR4 binds TF4 and, to a lesser extent, TF5, whereas TRAM is targeted by TF5. Next, we used coimmunoprecipitation (co-IP) to study if TF4 and TF5 disrupt binary interactions between TRIF and either TLR4 or

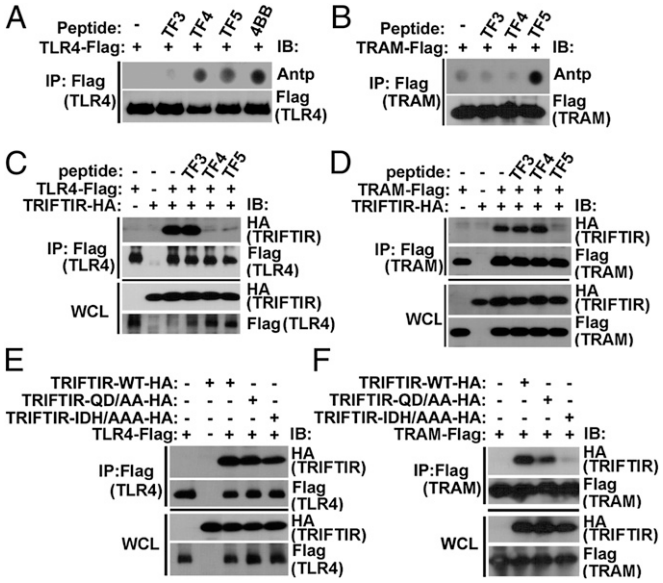

Fig. 3. TF5 targets TLR4 and TRAM and blocks TRIF interaction with TLR4 and TRAM, whereas TF4 is selective to TLR4 and blocks only TLR4–TRIF association (*A*–*D*). Mutations within the area represented by TF5 affect TRIF–TRAM, not TRIF–TLR4, association (*E* and *F*). (*A* and *B*) Extracts of HEK293T cells expressing Flag-tagged TLR4 or TRAM were incubated with peptides for 1 h and immunoprecipitated with anti-Flag antibody followed by dot blot assay with anti-Antp antibody. (*C* and *D*) HEK293T cells were transfected with plasmids as indicated. Forty-eight hours posttransfection, cells were treated with 20 μM of the indicated peptide for 1 h. Lysates were immunoprecipitated with anti-Flag antibody and the interacting complex was assessed using anti-HA antibody. (*E* and *F*) Residues Ile-448, Asp-449, and His-450 of TRIF are important for TRIF and TRAM association. We cotransfected 0.5 μg HA-tagged TRIF TIR plasmids with 10 μg Flag-tagged TLR4 or 1 μg Flag-tagged TRAM constructs into HEK293 cells. Protein complexes were immunoprecipitated with anti-Flag antibody and blotted with anti-HA antibody. The whole-cell lysates (WCLs) were used to control for the expression levels of TRIF TIR, TRAM, or TLR4 in *C*–*F*. Data in *A*–*F* represent one of three independent experiments.

TRAM. A plasmid that encodes an HA-tagged TIR domain of TRIF (TRIF TIR-HA) was transfected to HEK293T cells together with plasmids that encode Flag-tagged TLR4 or Flag-tagged TRAM, and the peptide effects on TRIF association with TLR4 and TRAM were studied by co-IP. Our data suggest that the TIR domain of TRIF can be coimmunoprecipitated with TLR4 and TRAM. Both inhibitory TRIF peptides block TRIF–TLR4 interaction, whereas the noninhibitory peptide TF3 had no effect. This observation is consistent with the observation that both peptides, TF4 and TF5, bind TLR4. Only the TF5 peptide, and not the TF4 peptide, blocked TRIF–TRAM association (Fig. 3*D*). This observation supports the dot blot data that show that only TF5, and not TF4, binds to TRAM (Fig. 3*B*). These data suggest that TF5 interacts with both TLR4 and TRAM TIRs and thereby can block a wider set of TIR–TIR interactions. Interestingly, neither TF4 nor TF5 bound to MyD88 or TIRAP TIR domains (Fig. S4 *A* and *B*).

Residues Ile-448, Asp-449, and His-450 Within Region 5 of TRIF TIR Are Important for TRIF–TRAM, Not TRIF–TLR4, Association. Our data demonstrate that TF5 potently inhibits TLR4 signaling (Fig. 1) and binds to both TRAM (Fig. 3*B*) and TLR4 (Fig. 3*A*). These findings suggest that the B helix of TRIF TIR might be a functionally important TIR–TIR interface. To confirm this hypothesis, we engineered two TRIF TIR variants in which two groups of residues within the B helix were substituted with alanine and studied how these mutations affect TRIF–TLR4 and TRIF–TRAM associations. The first mutant, designated as TRIF TIR-QD/AA, has Gln-445 and Asp-446 residues replaced by alanine. The second mutant, TRIF TIR-IDH/AAA, has Ile-448, Asp-449, and His-450 substituted with alanines. Although QD/AA substitution only weakly affected the binding of TRIF TIR to TLR4 or TRAM, the IDH/AAA substitution abolished the interaction between TRAM and TRIF, but not the TRIF–TLR4 interaction (Fig. 3 *E* and *F*). These data confirm that the B helix of TRIF TIR mediates the interaction of TRIF and TRAM TIR domains and indicate that residues Ile-448, Asp-449, and His-450, which are highly surface-exposed (Fig. S5, *Right*), are critical for TRAM and TRIF interaction. Additionally, TF45, a peptide that represents the border area between regions 4 and 5 and does not include the residues -IDH- (Table S1), does not inhibit TLR4 signaling (Fig. S6).

TF5 Blunts LPS-Induced Cytokine Response and Improves Survival of Mice After LPS Challenge. We next examined TF5 in vivo. C57BL/6J mice were treated with TF5 or CP (10 nmol/g mouse weight) i.p. (Fig. 4*A*) or i.v. (Fig. 4*B*) 1 h before administration of a nonlethal LPS dose (1 μg/g). Plasma TNF-α and IL-6 were measured immediately before and 1, 2, and 4 h after LPS administration. The i.p. administration of TF5 dramatically decreased systemic levels of TNF-α and IL-6 induced by a sublethal LPS dose throughout the observation period (Fig. 4*A*). The i.v. TF5 administration affected systemic cytokine levels less strongly than the i.p. administration; nevertheless, the effect of i.v. TF5 on circulating IL-6 at the 2 and 4 h time points was highly significant (Fig. 4*B*). We next studied whether TF5 would protect mice from a lethal LPS challenge. LPS (20 μg/g) was injected into animals

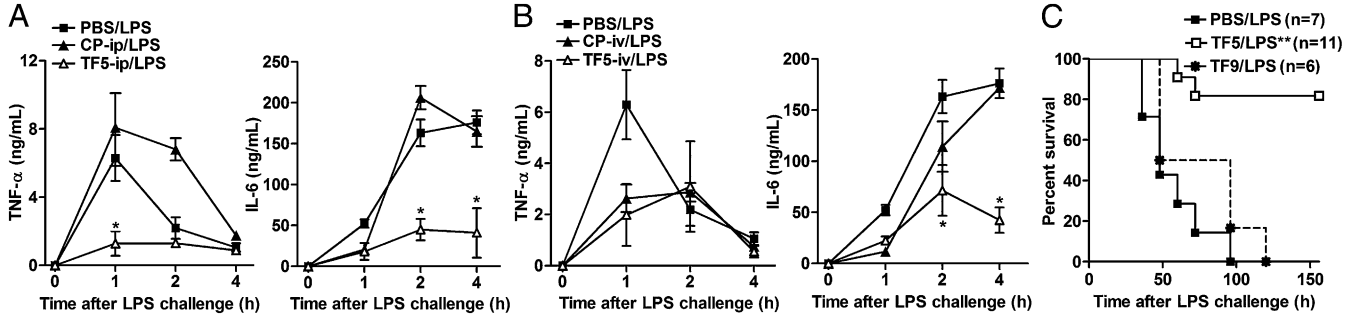

Fig. 4. TF5 suppresses LPS-induced cytokine activation in vivo and protects mice from lethal endotoxemia. (*A* and *B*) C57BL/6J mice were injected i.p. with a sublethal dose of purified *E. coli* K235 LPS (1 μg/g body weight), and plasma TNF-α and IL-6 levels were measured before and 1, 2, and 4 h after LPS challenge. Peptides (10 nmol/g) or PBS were injected i.p. (*A*) or i.v. (*B*) 1 h before LPS administration. The means ± SEM of values obtained from five plasma samples are shown. $*P < 0.01$. (*C*) Survival of C57BL/6J mice pretreated with peptides for 1 h and challenged with a lethal LPS dose (20 μg/g). TF9 was used as a noninhibitory CP. Significance of differences in survival rate was determined by the Mantel–Cox log-rank test using GraphPad Prism software. $**P < 0.001$.

i.p. This dose of LPS induced 100% mortality in control groups of mice (Fig. 4*C*). Pretreatment of mice with 10 nmol/g of TF5 rescued 9 of 11 mice challenged with the lethal LPS dose (Fig. 4*C*), whereas the noninhibitory TF9 peptide did not improve survival (Fig. 4*C*). The survival rate improvement in the TF5-treated group is highly significant compared with both control groups—that is, vehicle- (PBS-) and TF9-treated group ($P < 0.001$). The results presented demonstrate that TF5 effectively suppresses the systemic TLR4-mediated inflammation and validate peptides or peptidomimetics designed based on the structure of the B helix of TRIF TIR as drug candidates for the development of therapeutics for treatment of TLR4-driven septic shock.

Discussion

This study examines decoy peptides derived from the TIR domain of the TLR adapter TRIF and thereby extends our prior work that examined sets of similarly designed peptides from TLR4, TRAM, and TIRAP (20–22). Two TRIF peptides, TF4 and TF5, which, based on structural alignments, are derived from the BB loop and the B helix, the region immediately following the BB loop, inhibit TLR4 signaling. The BB loop peptide was identified previously as a moderately inhibitory peptide compared with peptides derived from the BB loop of the four TLR4 adapters (24). The sequence of the newly identified inhibitory TF5 peptide is not similar to any decoy peptide previously identified by us or others as a TLR4 inhibitor (20–22, 32–34). One example of dissimilarity of inhibitory sequences is the peptides derived from region 5 of TIRAP (ELCQALSRSHCR) (21) and TRIF (CLQDAIDHSGFT) that have only three amino acids positioned identically. Divergence of inhibitory sequences has long been recognized (19) and stems from dissimilarity of surface-exposed residues in TIR domains (35). It should also be noted that region 5 is largely helical in the resolved structures of TIR domains of TLR2 (13), TLR1 (13), TLR10 (36), and IL-1RAPL (37), whereas the MyD88 TIR has a shorter helix B (38) and the homologous region of TIRAP/Mal does not form a helix (14, 15).

Each set of TIR decoy peptides we have examined contained several peptides that potently inhibit TLR4 signaling. The inhibitory peptides derive from different structural regions of TIR domains. For example, the BB loop peptides (region 4) from TLR4, TRAM, and TRIF TIR domains are inhibitory, whereas in the TIRAP set, peptides derived from the flanking regions, TR3 and TR5 peptides, are more potent inhibitors (21). Peptides from region 5 were inhibitory in TIRAP and TRIF libraries, not in TLR4 or TRAM libraries, whereas in the TRAM library, the C helix peptide (region 6), but not B helix peptide, was inhibitory. These findings reflect and support the generalization that positions of TIR–TIR interaction sites are not conserved among TIR domains (19).

The peptide binding assay has demonstrated that the TRIF B helix peptide, TF5, binds to both TRAM and TLR4, whereas the BB loop peptide, TF4, is more selective and binds to TLR4, but not TRAM (Fig. 3 *A* and *B*). In full accordance with this binding pattern, TF5 blocked interactions of TRIF with both TRAM and TLR4 in co-IP assays, whereas TF4 affected TRIF–TLR4 but not TRIF–TRAM interaction (Fig. 3 *C* and *D*). Alanine substitutions introduced into the TRIF TIR region that corresponds to TF5, however, affected TRIF co-IP more selectively than the TF5 blocking peptide. The replacement of -IDH- residues located in the center of TF5 with alanines abolished TRIF–TRAM co-IP, whereas this mutation had little or no effect on TRIF–TLR4 interaction (Fig. 3 *E* and *F*). This strong and selective effect of these residues on TRIF–TRAM interaction, further supported by the ability of the corresponding peptide to block this protein interaction, suggests that the B helix of TRIF is a part of the functional TRIF–TRAM interface. Replacement of -QD- residues, which are located in the B helix coil, which precedes the IDH site, did not significantly affect the TRIF–TRAM co-IP, indicating a lesser contribution of these amino acids to TRIF–TRAM recognition and binding. Collectively, our binding studies suggest that the folded TRIF binds TRAM through the B helix of TRIF TIR, whereas TRIF–TLR4 interaction is likely mediated by the BB loop of TRIF TIR. The peptide derived from the B helix of TRIF, TF5, however, can bind to both TRAM and TLR4 and thereby block both TRIF–TRAM and TRIF–TLR4 interaction. Thus, TF5 binding to TLR4 appears to represent an example of a peptide derived from a protein–protein interface that has a wider set of binding partners compared with the same peptide sequence in the context of the folded protein. Less specific binding and higher affinity of a peptide–protein interaction (compared with that of the protein–protein interaction) might be due to higher conformation flexibility of peptides and was anticipated for some cases (19). Although binding of TF5 to TLR4 is unlikely to represent a functionally important TIR–TIR interaction, the ability of TF5 to bind to TLR4 and block an additional interaction of TIR domains may be a critical factor that makes this peptide a good inhibitor in wild-type cells and in vivo. We think that the finding that TF5 has multiple binding partners among TIR domains of proteins that mediate TLR4 signal transduction is very important for understanding the mechanisms of signaling inhibition by decoy peptides.

In wild-type macrophages, TRIF peptides, similarly to inhibitory peptides from other TIR domains that we identified previously (20–22), inhibit cytokine genes traditionally associated with the TRIF-dependent, as well as the TRIF-independent, MyD88-dependent pathway (Fig. 1). However, TF5 did not block the MyD88-dependent responses in TRIF-deficient iBMDMs (Fig. 2 *F* and *H*). This finding strongly confirms that direct binding of TF5 to TRAM is the key mechanism of TLR4 inhibition by TF5. The ability of TF5 to block the MyD88-dependent genes in wild-type cells, but not in TRIF-deficient cells, in our opinion, is not controversial because these TRIF- and MyD88-dependent pathways that were first identified based on observations obtained using gene knockout models activate significantly overlapping sets of transcription factors and genes (4, 9, 39, 40), and therefore, both pathways—that is, all four adapters—are important for full activation of cytokine genes in wild-type cells. Targeting the MyD88-dependent genes in wild-type cells by TRIF peptides can also be explained by the fact that both peptides bind TLR4 (Fig. 3*A*) and thereby can interfere with recruitment of adapters of the MyD88-dependent pathway. Interestingly, viral inhibitory peptide of TLR4 (VIPER) also demonstrates broad inhibitory specificity, as this peptide blocks LPS-induced activation of TNF-α, macrophage inflammatory protein 2 (MIP-2), RANTES, and IL-6 in iBMDMs (34).

TF5, the more potent TLR4-inhibitory TRIF peptide in vitro, was examined in vivo. TF5 potently diminished systemic LPS-induced cytokine response (Fig. 4*A*). In survival tests, TF5 rescued more than 80% of animals injected with an LPS dose that caused 100% mortality in the control group (Fig. 4*C*). Efficiency of TF5 administered i.p. was higher than that after i.v. administration. A similar pattern was noted previously for TM4 and TM4-ΔC; these two TRAM-derived peptides also provided more efficient anti-inflammatory protection after i.p. administration (22). Results of in vivo experiments demonstrate that TF5 effectively suppresses the systemic TLR4-mediated inflammation and thus validate peptides or peptidomimetic designed based on the structure of B helix of TRIF TIR as drug candidates for development of therapeutics for treatment of TLR4-driven septic shock.

In summary, this study identifies TRIF TIR domain-derived peptides that effectively block TLR4 signaling in vivo. Our data suggest that TLR4 adapters TRIF and TRAM interact through the B helix of TRIF.

Materials and Methods

Mice, Cells, and Treatment. C57BL/6J mice, including the MyD88-deficient strain, were obtained from the Jackson Laboratory. Harvesting, culturing, and stimulation of peritoneal macrophages were described previously (24). THP-1 cells were cultured in 10% (vol/vol) FCS cRPMI-1640 and differentiated by 3 d

incubation in the presence of 10 nM phorbol myristate acetate (PMA). Immortalized wild-type and TRIF-deficient BMDM were a kind gift of Kate Fitzgerald (University of Massachusetts Medical School, Worcester, MA). Highly purified *Escherichia coli* K235 LPS (41) was used at the final concentration of 100 ng/mL in cell culture experiments. We also used 2,3-bis(palmitoyloxy)-(2-RS)-propyl-*N*-palmitoyl-(R)-Cys-Ser-Lys4-OH (P3C) and S-[2,3-bis (palmitoyloxy)-(2-RS)-propyl]-[R]-Cys-Ser-Lys4-OH (P2C) (EMC Microcollections). ODN 1668 and low molecular weight polyinosinic-polycytidylic acid [poly (I:C)] in complex with LyoVecTM were obtained from InVivoGen.

Expression Vectors. Full-length TLR4-Flag, TRAM-Flag, or the TRIF TIR-HA constructs were generated by PCR amplification of mouse TLR4, TRAM, or the TIR domain of mouse TRIF cDNA and cloned into the pEF-BOS vector with C-terminal Flag or HA tag. MyD88 TIR-Cer and TIRAP-Cer plasmids were made by PCR amplification of mouse MyD88 or TIRAP cDNA and cloning into the mTLR4-Cer construct (20) by replacing the TLR4 coding sequence. The alanine substitutions in TRIF TIR were generated by site-directed mutagenesis using the kit from Agilent Technologies, Inc.

Immunoblotting and Co-IP. HEK293T cells were transfected using Superfect Transfection Reagent (Qiagen) and lysed 48 h posttransfection as described previously (22). Rabbit antibody against phospho-ERK, phospho-JNK, STAT1-Y701, total STAT1, and GAPDH were from Cell Signaling Technology. Rabbit anti–phospho-p38 antibody was from Promega. Mouse anti-Flag M2 and rabbit anti-HA antibodies were from Sigma-Aldrich.

Dot Blot Analysis of Peptide–Protein Binding. We transiently transfected 2×10^6 HEK293T cells with 10 μg TLR4-Flag, or 1 μg TRAM-Flag, MyD88 TIR-Cer, or TIRAP-Cer construct. Cells were lysed 48 h posttransfection, and lysate aliquots containing 100 μg of total protein were diluted by PBS to 500 μL and incubated with or without peptides (20 μM) for 1 h at 4 °C, followed by 3 h incubation with 0.5 μg of mouse anti-Flag or anti-eCFP antibody (8A6, Origene) and 4 h incubation with 25 μL protein G Agarose beads (Roche). The beads were then washed four times and boiled in Laemmli buffer. The supernatants were then spotted into the PVDF membrane, followed by immunoblotting with anti-Antp antibody (Abcam).

Animal Experiments. Eight-week-old C57BL/6J mice were injected i.p. with *E. coli* K235 LPS (1 or 20 μg/g of animal weight). Peptides were administered 1 h before LPS. Survival of animals was monitored every 6–16 h after LPS challenge. All animal experiments were carried out with University of Maryland School of Medicine Office of Animal Welfare Assurance approval.

A full description of cytokine mRNA and protein quantification, MTT viability assay, and CD spectroscopy methods as well as detailed peptide information are provided in *SI Materials and Methods*.

ACKNOWLEDGMENTS. We thank Dr. Wendy Lai for ELISA measurement of IFN-β. This work was supported by National Institutes of Health (NIH) Grants AI-082299 (to V.Y.T.) and AI-018797 (to S.N.V.). K.H.P. is supported by NIH T32 Grant AI-095150.

1. Hoshino K, et al. (1999) Cutting edge: Toll-like receptor 4 (TLR4)-deficient mice are hyporesponsive to lipopolysaccharide: Evidence for TLR4 as the Lps gene product. *J Immunol* 162(7):3749–3752.
2. Poltorak A, et al. (1998) Defective LPS signaling in C3H/HeJ and C57BL/10ScCr mice: Mutations in Tlr4 gene. *Science* 282(5396):2085–2088.
3. Medzhitov R, et al. (1998) MyD88 is an adaptor protein in the hToll/IL-1 receptor family signaling pathways. *Mol Cell* 2(2):253–258.
4. Horng T, Barton GM, Flavell RA, Medzhitov R (2002) The adaptor molecule TIRAP provides signalling specificity for Toll-like receptors. *Nature* 420(6913):329–333.
5. Fitzgerald KA, et al. (2001) Mal (MyD88-adapter-like) is required for Toll-like receptor-4 signal transduction. *Nature* 413(6851):78–83.
6. Yamamoto M, et al. (2002) Cutting edge: A novel Toll/IL-1 receptor domain-containing adapter that preferentially activates the IFN-beta promoter in the Toll-like receptor signaling. *J Immunol* 169(12):6668–6672.
7. Oshiumi H, Matsumoto M, Funami K, Akazawa T, Seya T (2003) TICAM-1, an adaptor molecule that participates in Toll-like receptor 3-mediated interferon-beta induction. *Nat Immunol* 4(2):161–167.
8. Oshiumi H, et al. (2003) TIR-containing adapter molecule (TICAM)-2, a bridging adapter recruiting to toll-like receptor 4 TICAM-1 that induces interferon-beta. *J Biol Chem* 278(50):49751–49762.
9. Fitzgerald KA, et al. (2003) LPS-TLR4 signaling to IRF-3/7 and NF-kappaB involves the toll adapters TRAM and TRIF. *J Exp Med* 198(7):1043–1055.
10. Pålsson-McDermott EM, O'Neill LA (2004) Signal transduction by the lipopolysaccharide receptor, Toll-like receptor-4. *Immunology* 113(2):153–162.
11. Kagan JC, et al. (2008) TRAM couples endocytosis of Toll-like receptor 4 to the induction of interferon-beta. *Nat Immunol* 9(4):361–368.
12. Rock FL, Hardiman G, Timans JC, Kastelein RA, Bazan JF (1998) A family of human receptors structurally related to Drosophila Toll. *Proc Natl Acad Sci USA* 95(2):588–593.
13. Xu Y, et al. (2000) Structural basis for signal transduction by the Toll/interleukin-1 receptor domains. *Nature* 408(6808):111–115.
14. Valkov E, et al. (2011) Crystal structure of Toll-like receptor adaptor MAL/TIRAP reveals the molecular basis for signal transduction and disease protection. *Proc Natl Acad Sci USA* 108(36):14879–14884.
15. Lin Z, Lu J, Zhou W, Shen Y (2012) Structural insights into TIR domain specificity of the bridging adaptor Mal in TLR4 signaling. *PLoS ONE* 7(4):e34202.
16. Dunne A, Ejdeback M, Ludidi PL, O'Neill LA, Gay NJ (2003) Structural complementarity of Toll/interleukin-1 receptor domains in Toll-like receptors and the adaptors Mal and MyD88. *J Biol Chem* 278(42):41443–41451.
17. Núñez Miguel R, et al. (2007) A dimer of the Toll-like receptor 4 cytoplasmic domain provides a specific scaffold for the recruitment of signalling adaptor proteins. *PLoS ONE* 2(8):e788.
18. Monie TP, Moncrieffe MC, Gay NJ (2009) Structure and regulation of cytoplasmic adapter proteins involved in innate immune signaling. *Immunol Rev* 227(1):161–175.
19. Toshchakov VY, Vogel SN (2007) Cell-penetrating TIR BB loop decoy peptides a novel class of TLR signaling inhibitors and a tool to study topology of TIR-TIR interactions. *Expert Opin Biol Ther* 7(7):1035–1050.
20. Toshchakov VY, Szmacinski H, Couture LA, Lakowicz JR, Vogel SN (2011) Targeting TLR4 signaling by TLR4 Toll/IL-1 receptor domain-derived decoy peptides: Identification of the TLR4 Toll/IL-1 receptor domain dimerization interface. *J Immunol* 186(8):4819–4827.
21. Couture LA, Piao W, Ru LW, Vogel SN, Toshchakov VY (2012) Targeting Toll-like receptor (TLR) signaling by Toll/interleukin-1 receptor (TIR) domain-containing adapter protein/MyD88 adapter-like (TIRAP/Mal)-derived decoy peptides. *J Biol Chem* 287(29):24641–24648.
22. Piao W, Vogel SN, Toshchakov VY (2013) Inhibition of TLR4 signaling by TRAM-derived decoy peptides in vitro and in vivo. *J Immunol* 190(5):2263–2272.
23. Derossi D, Joliot AH, Chassaing G, Prochiantz A (1994) The third helix of the Antennapedia homeodomain translocates through biological membranes. *J Biol Chem* 269(14):10444–10450.
24. Toshchakov VU, Basu S, Fenton MJ, Vogel SN (2005) Differential involvement of BB loops of toll-IL-1 resistance (TIR) domain-containing adapter proteins in TLR4- versus TLR2-mediated signal transduction. *J Immunol* 175(1):494–500.
25. Toshchakov V, et al. (2002) TLR4, but not TLR2, mediates IFN-beta-induced STAT1alpha/beta-dependent gene expression in macrophages. *Nat Immunol* 3(4):392–398.
26. Berlose JP, Convert O, Derossi D, Brunissen A, Chassaing G (1996) Conformational and associative behaviours of the third helix of antennapedia homeodomain in membrane-mimetic environments. *Eur J Bioch* 242(2):372–386.
27. Czajlik A, Mesko E, Penke B, Perczel A (2002) Investigation of penetratin peptides. Part 1. The environment dependent conformational properties of penetratin and two of its derivatives. *J Pept Sci* 8(4):151–171.
28. Christiaens B, et al. (2002) Tryptophan fluorescence study of the interaction of penetratin peptides with model membranes. *Eur J Biochem* 269(12):2918–2926.
29. Andrade MA, Chacón P, Merelo JJ, Morán F (1993) Evaluation of secondary structure of proteins from UV circular dichroism spectra using an unsupervised learning neural network. *Protein Eng* 6(4):383–390.
30. Sreerama N, Woody RW (1993) A self-consistent method for the analysis of protein secondary structure from circular dichroism. *Anal Biochem* 209(1):32–44.
31. Finkelstein A, Ptitsyn O (2002) *Protein Physics: A Course of Lectures* (Academic, San Diego), p 354.
32. Toshchakov VY, Fenton MJ, Vogel SN (2007) Cutting Edge: Differential inhibition of TLR signaling pathways by cell-permeable peptides representing BB loops of TLRs. *J Immunol* 178(5):2655–2660.
33. Snyder GA, et al. (2013) Molecular mechanisms for the subversion of MyD88 signaling by TcpC from virulent uropathogenic Escherichia coli. *Proc Natl Acad Sci USA* 110(17):6985–6990.
34. Lysakova-Devine T, et al. (2010) Viral inhibitory peptide of TLR4, a peptide derived from vaccinia protein A46, specifically inhibits TLR4 by directly targeting MyD88 adaptor-like and TRIF-related adaptor molecule. *J Immunol* 185(7):4261–4271.
35. Slack JL, et al. (2000) Identification of two major sites in the type I interleukin-1 receptor cytoplasmic region responsible for coupling to pro-inflammatory signaling pathways. *J Biol Chem* 275(7):4670–4678.
36. Nyman T, et al. (2008) The crystal structure of the human toll-like receptor 10 cytoplasmic domain reveals a putative signaling dimer. *J Biol Chem* 283(18):11861–11865.
37. Khan JA, Brint EK, O'Neill LA, Tong L (2004) Crystal structure of the Toll/interleukin-1 receptor domain of human IL-1RAPL. *J Biol Chem* 279(30):31664–31670.
38. Ohnishi H, et al. (2009) Structural basis for the multiple interactions of the MyD88 TIR domain in TLR4 signaling. *Proc Natl Acad Sci USA* 106(25):10260–10265.
39. Kawai T, Adachi O, Ogawa T, Takeda K, Akira S (1999) Unresponsiveness of MyD88-deficient mice to endotoxin. *Immunity* 11(1):115–122.
40. Björkbacka H, et al. (2004) The induction of macrophage gene expression by LPS predominantly utilizes Myd88-independent signaling cascades. *Physiol Genomics* 19(3):319–330.
41. McIntire FC, Sievert HW, Barlow GH, Finley RA, Lee AY (1967) Chemical, physical, biological properties of a lipopolysaccharide from Escherichia coli K-235. *Biochemistry* 6(8):2363–2372.

Supporting Information

Piao et al. 10.1073/pnas.1313575110

SI Materials and Methods

Peptide Synthesis and Reconstitution. Peptides were obtained through the Biopolymer and Genomics Core Facility (University of Maryland, Baltimore). All peptides were >95% purity and quantified by spectrophotometry (1). Peptide sequences are shown in Table S1.

Quantitative Real-Time RT-PCR. Total RNA was isolated with Nucleospin RNA II kits (Macherey-Nagel, Inc.) followed by DNase treatment. cDNA was synthesized from 1 μg of RNA using Goscript transcriptase (Promega) and subjected to real-time PCR with gene-specific primers for HPRT, TNF-α, IL-1β, IFN-β, and RANTES (2) using H7900 ABI system and Fast SYBR-Green master mix (Applied Biosystems).

Cytokine ELISA. We plated 1×10^6 peritoneal macrophages in 24-well plates and treated them with peptides for 30 min before LPS stimulation. TNF-α, IL-6, IFN-β, and RANTES in cell supernatants, or IL-1β in cell lysates, were measured using ELISA kits from Biolegend and R&D Systems.

3-(4,5-Dimethylthiazol-2-yl)-2,5-diphenyltetrazolium bromide Viability Assay. We plated 5×10^4 mouse peritoneal macrophages into 96-well tissue culture plates, incubated them overnight, and treated them with peptides with or without LPS for 2 h, followed by a 3 h incubation with MTT [3-(4,5-Dimethylthiazol-2-yl)-2,5-diphenyltetrazolium bromide] (Sigma-Aldrich) at 0.5 mg/mL, and 50 μL DMSO was added to cells before reading OD at 540 nm.

CD Spectroscopy. CD spectroscopy was performed using the JASCO 810 spectrophotometer. Peptide CD spectra were taken at 50 μM peptide concentration in buffer containing 25 mM Na_2PO_4 and 25 mM NaCl (pH 6.0) at 25 °C. The spectra were taken in a 190–260 nm wavelength range with a 2 nm band gap. The spectra were averaged over at least six measurements. The analysis of peptide secondary structures was performed with the aid of Dichroweb (3).

1. Pace CN, Vajdos F, Fee L, Grimsley G, Gray T (1995) How to measure and predict the molar absorption coefficient of a protein. *Protein Sci* 4(11):2411–2423.
2. Couture LA, Piao W, Ru LW, Vogel SN, Toshchakov VY (2012) Targeting Toll-like receptor (TLR) signaling by Toll/interleukin-1 receptor (TIR) domain-containing adapter protein/MyD88 adapter-like (TIRAP/Mal)-derived decoy peptides. *J Biol Chem* 287(29):24641–24648.
3. Whitmore L, Wallace BA (2008) Protein secondary structure analyses from circular dichroism spectroscopy: Methods and reference databases. *Biopolymers* 89(5):392–400.

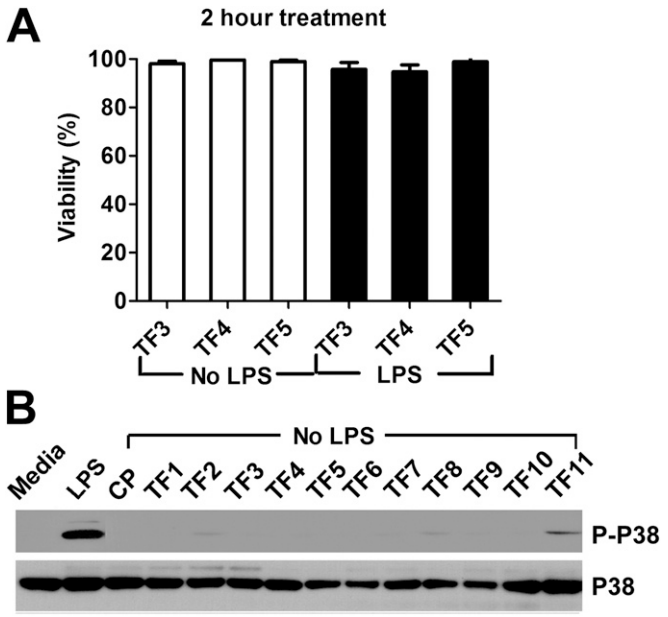

Fig. S1. Inhibitory Toll/IL-1R resistance (TIR) domain–containing adapter-inducing IFN-β (TRIF) peptides do not affect cell viability and do not activate p38. Mouse macrophages were incubated with the indicated peptides (20 μM) for 30 min, followed by LPS stimulation (100 ng/mL) for 2 h (*A*) or 30 min (*B*). (*A*) Cell viability was determined using MTT incorporation assay. (*B*) Cell extracts were immunoblotted for p38 phosphorylation and expression. Data represent two independent experiments.

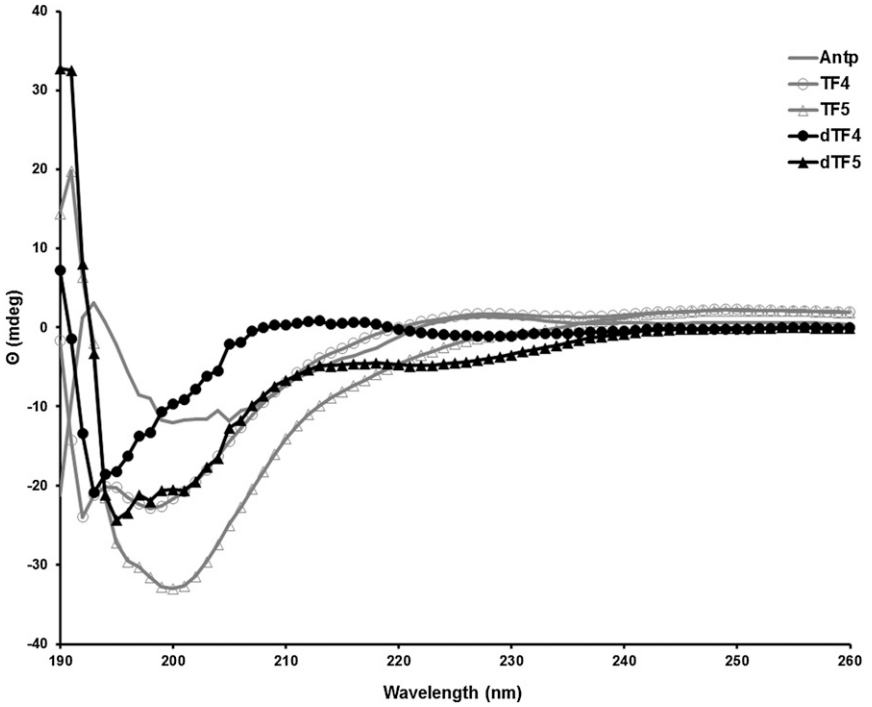

Fig. S2. CD spectra of TLR4-inhibitory, TRIF-derived peptides. The *Antennapedia* internalization sequence (Antp) spectrum (shown as a solid gray line) was used as a reference to calculate spectra of TRIF-specific sequences in TF4 and TF5. CD spectrum of TF4 is marked by hollow gray circles; the TF5 spectrum is shown by hollow black triangles. The referenced spectra of decoy sequences of TF4 and TF5 (dTF4 and dTF5) are shown as solid gray circles and solid black triangles, respectively.

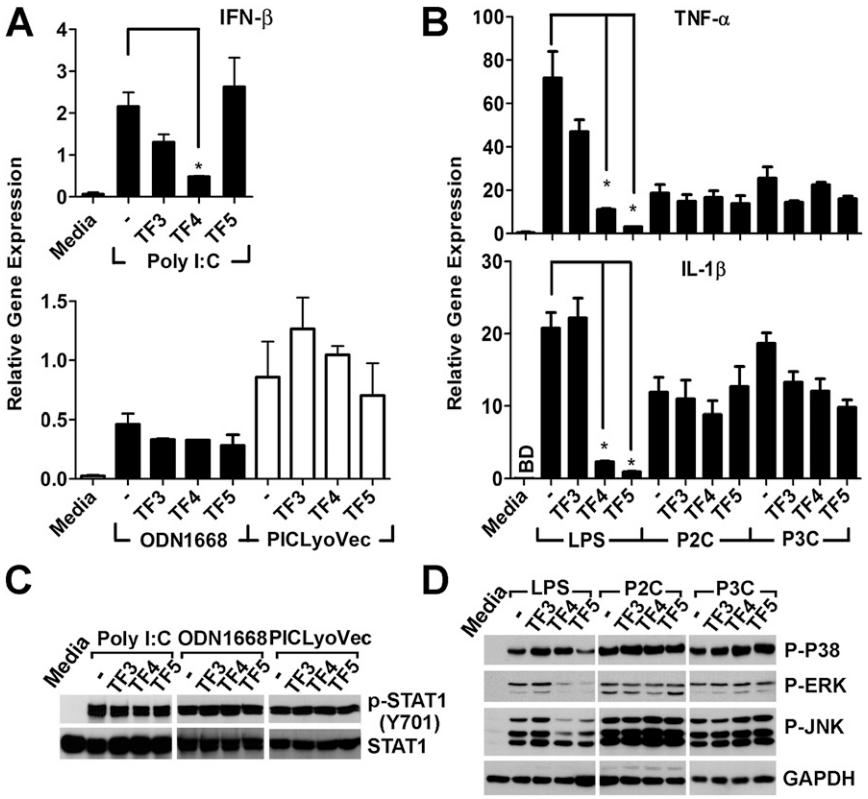

Fig. S3. TF5 inhibits TLR4 but not TLR2, TLR3, TLR9, or RIG-I–like receptors. Experimental details are as in Fig. 1. Peptides were used at 20 μM. Poly (I:C) was used at 50 μg/mL, oligonucleotide (ODN) 1668 at 2.5 μM, poly (I:C) LyoVec at 400 ng/mL, LPS at 100 ng/mL, and P2C at 50 and P3C at 500 ng/mL. (*A* and *B*) TLR3, TLR9, and retinoic acid-inducible gene 1 (RIG-I)–like receptor agonists, poly (I:C)–, ODN 1668–, and poly (I:C) LyoVec–induced IFN-β mRNA were measured 5 h after stimulation. TLR2-induced TNF-α and IL-1β mRNA were measured 1 h after stimulation. Means ± SEM of three independent experiments are shown. $*P < 0.01$. (*C*) STAT1-Y701 activation was measured after incubation of cells with poly (I:C) for 3 h, ODN 1668 for 5 h, or with poly (I:C) LyoVec for 16 h. (*D*) MAPK activation was measured 30 min after LPS or P3C stimulation and 15 min after P2C stimulation. Data in *C* and *D* represent three independent experiments.

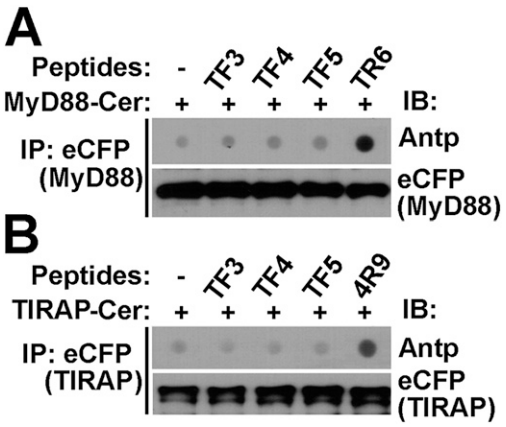

Fig. S4. TRIF peptides do not bind to the MyD88 or TIRAP TIR domain. Extracts of HEK293T cells that overexpress Cerulean-tagged MyD88 TIR domain (MyD88-Cer) (*A*) or TIRAP (TIRAP-Cer) (*B*) were incubated with the indicated peptide for 1 h at 4 °C and immunoprecipitated with mouse anti-CFP antibody followed by the dot blot assay using rabbit anti-Antp antibody. TIRAP-derived peptide TR6 (1) and TLR4-derived 4R9 peptide (2) were used as positive binding controls for their respective proteins. A representative blot of three independent experiments is shown.

1. Couture LA, Piao W, Ru LW, Vogel SN, Toshchakov VY (2012) Targeting Toll-like receptor (TLR) signaling by Toll/interleukin-1 receptor (TIR) domain-containing adapter protein/MyD88 adapter-like (TIRAP/Mal)-derived decoy peptides. *J Biol Chem* 287(29):24641–24648.
2. Toshchakov VY, Szmacinski H, Couture LA, Lakowicz JR, Vogel SN (2011) Targeting TLR4 signaling by TLR4 Toll/IL-1 receptor domain-derived decoy peptides: identification of the TLR4 Toll/IL-1 receptor domain dimerization interface. *J Immunol* 186(8):4819–4827.

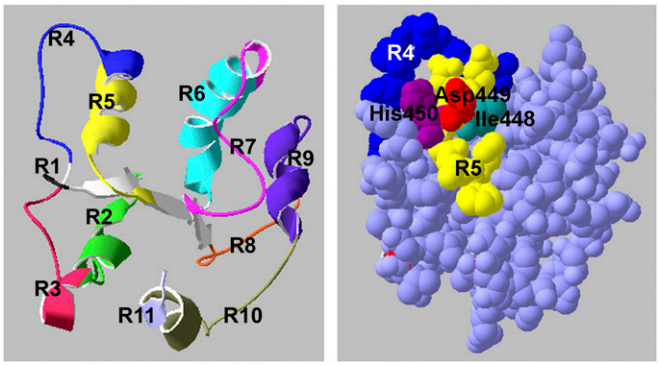

Fig. S5. Relative positions of TRIF TIR regions corresponding to the 11 decoy peptides (*Left*) and the surface-exposed residues of the B helix (*Right*). Surface regions represented by TF4 (blue) and TF5 (yellow) are highlighted in color. Ile-448 is shown in cyan, Asp-449 in red, and His-450 in purple. Images were produced using the DeepView viewer. The coordinate file for the human TRIF TIR model was kindly provided by Wei Tiandi (Shandong University, Jinan, China) (1).

1. Wu B, Xin B, Jin M, Wei T, Bai Z (2011) Comparative and phylogenetic analyses of three TIR domain-containing adaptors in metazoans: Implications for evolution of TLR signaling pathways. *Dev Comp Immunol* 35(7):764–773.

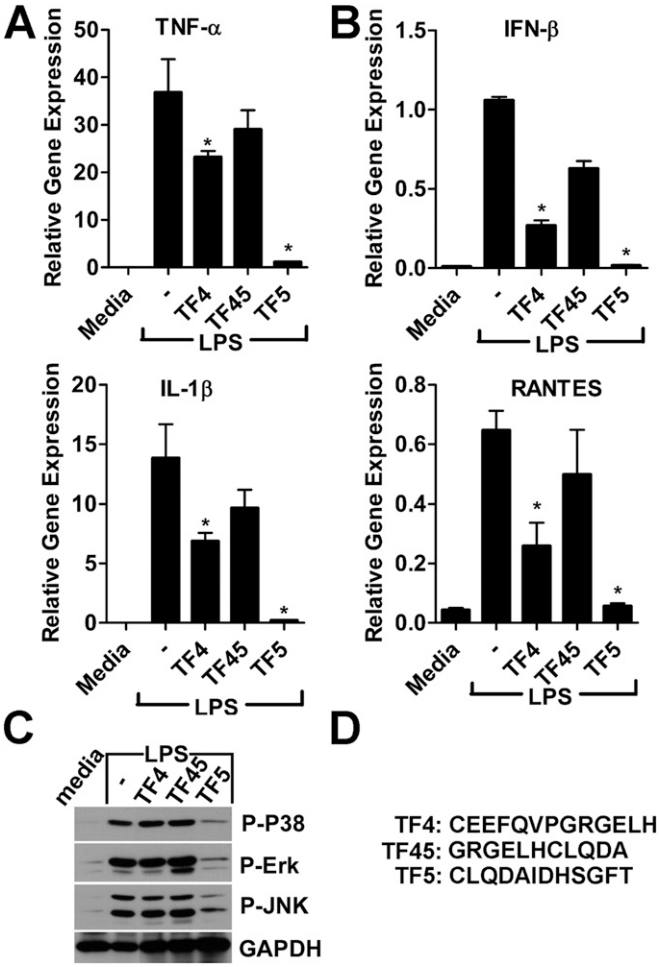

Fig. S6. Peptide TF45 that overlaps with TF4 and TF5 does not suppress TLR4-mediated macrophage activation. Experimental details are as in Fig. 1. We preincubated 2×10^6 mouse peritoneal macrophages with 20 μM of the indicated peptide for 30 min and stimulated them with LPS (100 ng/mL). (*A* and *B*) LPS-induced cytokine mRNA expression was measured 1 h after stimulation. Means ± SEM of three independent experiments are shown. $^*P < 0.01$. (*C*) Cell extracts for MAPKs activation were collected 30 min after LPS stimulation. Data represent three separate experiments. The sequences of murine TF4, TF45, and TF5 are presented in *D*.

Table S1. Sequences of decoy peptides*

Peptide name	Peptide sequence	Putative structural region
TF1	VLDHSETSDQKFYN	Segment preceding βA†
TF2	ARADEQVARIREK	AA and αA
TF3	ETLGVPDGAT	αA, AB, and BB
TF4	CEEFQVPGRGELH	BB and αB
TF45	GRGELHCLQDA	αB
TF5	CLQDAIDHSGFT	αB and BC
TF5-ΔC	CLQDAIDHS	αB
hTF5	CLQDAIDHSAFI	αB and BC
TF6	ASFDCSLSLHQINH	CC and αC
TF7	ALMNSLTQSGRQDC	CD and βD
TF8	LPLECSQAQL	DD
TF9	SPDTTRLLHSIVW	DD and αD
TF10	LDEHSPIFARKVA	EE and αE
TF11	NTFKTQKLQAQRV	αE
CP	SLHGRGDPMEAFII	Randomized sequence

*Only decoy sequences of peptides are shown. Each peptide also has a "constant" part comprising the cell-permeating sequence of the *Antennapedia* homeodomain (RQIKIWFQNRRMKWKK) placed at the N terminus of the decoy sequence.

†Structural regions of TIR domain are designated as follows: helices are designated by α—for example, αA, helix A; strands are indicated by β; loops are indicated by two capital letters—for example, AA, loop that connects strand A and helix A.